Scientia Iranica A (2013) 20 (2), 242–250

Sharif University of Technology

Scientia Iranica

Transactions A: Civil Engineering

www.sciencedirect.com

Prediction of liquefaction induced lateral displacements using robust optimization model

F. Kalantary [a,*], H. MolaAbasi [b], M. Salahi [c], M. Veiskarami [d]

[a] *School of Civil Engineering, Khajeh Nasir Toosi University of Technology, Iran*
[b] *Faculty of Engineering, Babol University of Technology, Iran*
[c] *Faculty of Mathematical Sciences, University of Guilan, Iran*
[d] *Faculty of Engineering, University of Guilan, Iran*

Received 4 April 2012; revised 31 July 2012; accepted 23 December 2012

KEYWORDS

Least squares;
Robust optimization;
Second order cone;
Soil liquefaction;
Earthquake;
Lateral displacement.

Abstract Lateral spreading and flow failure are amongst the most destructive effects of liquefaction. Estimation of the hazard of lateral spreading requires characterization of subsurface conditions, principally soil density, fine content, groundwater conditions, site topography and seismic characteristics. However, inaccuracies in the measurement or estimation of the influencing parameters have always been a major concern and, thus, various statistical approaches have been improvised to subdue the effect of such inaccuracies in the prediction of future events.

Very few empirical correlations consider the effect of uncertainties in predicting the extent of lateral movement. Hence, in this article, an innovative approach, based on robust optimization, has been utilized to enumerate the effect of such uncertainties. In order to assess the merits of the proposed approach, a database containing 526 data points of liquefaction-induced lateral ground spreading case histories from eighteen different earthquakes, is used.

The identification technique used in this article is based on the robust counterpart of the least squares problem, which is a second order cone problem, and is efficiently solved by the interior point method. A definition of uncertainty, based on the Frobenius norm of the data, is introduced and examined against the correlation coefficients for various empirical models, including a new linear model, and, thereby, optimum values are determined.

The results suggest that in comparison with Al Bawwab models, the robust method is a better pattern recognition tool for datasets with degrees of uncertainty. It is further shown that logarithmic correlations perform better in deterministic valuation, whereas, considering uncertainty, they give similar degrees of accuracy to the new linear model.

1. Introduction

Liquefaction occurs in saturated sand deposits, due to excess pore water pressure increase, during earthquake induced cyclic shear stresses. It can cause serious to destructive damage to structures. The liquefaction mechanism includes ground subsidence, flow failure and lateral spreading, among other effects. Perhaps one of the earliest observed cases of lateral spreading is the San Francisco 1906 earthquake [1]. Lateral spreading involves the movement of relatively intact soil blocks on a layer of liquefied soil toward a free face or incised channel. It can also induce different forms of ground deformation, which can be very destructive, in the vicinity of natural and artificial slopes.

A number of approaches have been proposed for prediction of the magnitude of lateral ground displacements under different conditions. Al Bawwab [2] has categorized the methods into the following four groups:

(1) Numerical analyses in the form of finite element and/or finite difference techniques;

* Corresponding author. Tel.: +98 912 1069256; fax: +98 21 77245305.
E-mail addresses: fz_kalantary@knt.ac.ir (F. Kalantary), hma@stu.nit.ac.ir (H. MolaAbasi), salahim@guilan.ac.ir (M. Salahi), mveiskarami@shirazu.ac.ir (M. Veiskarami).

Peer review under responsibility of Sharif University of Technology.

Production and hosting by Elsevier

1026-3098
http://dx.doi.org/10.1016/j.scient.2012.12.025

Nomenclature

D_H	Horizontal displacement
$D50_{15}$	Average grain size for granular materials within T_{15}
F_{15}	Average fines content (finer than 75 lm) for granular materials included within T_{15}
H	Average thickness of the liquefied layer
L	Distance to the free face from the point of displacement
LSI	Liquefaction severity index
M_W	Earthquake moment magnitude
$(N1)60$	Corrected standard penetration test (SPT) blow count number
R	Nearest horizontal distance of the seismic energy source to the site
R^*	Distance coefficient that is a function of earthquake magnitude
R^2	Coefficient of determination
S	Slope of ground surface
T	Average thickness of the liquefied surface layer
T_{15}	Cumulative thickness of saturated cohesion-less soil layers with corrected SPT number $(N1)60$ less than 15
W	Free face ratio
$a_{\max}$	Maximum horizontal ground acceleration
β	Ground surface slope angle
$\varphi' eqv, liq$	The equivalent mobilized angle of internal friction of liquefied
a_y	Yield acceleration
z_{cr}	Critical potentially liquefiable soil sub-layer depth
ε	Model correction term
θ_i, b_i	Constant of equations obtained empirically

(2) Simplified analytical methods;
(3) Soft computing techniques, and
(4) Empirical methods, developed, based on the assessment of either laboratory test data or statistical analyses of lateral spreading case histories.

However, viewing the approaches based on their basic inputs, the approaches may be classified into the categories shown in Figure 1.

However, all predictions based on any of the aforementioned approaches require determination of input parameters, which are prone to uncertainties and inaccuracies. The effect of any inaccuracies of input data in the numerical and analytical approach may be studied by a sensitivity analysis of the predictions on various input data. Due to versatility, empirical and semi-empirical correlations remain at the center of the practice [1,2]. Some advanced forms of multi-linear regression analysis or various forms of identification techniques have been combined with empirical methods to arrive at better evaluations of model parameters [3].

In this paper, a different approach to quantify the effect of uncertainties on the evaluation of model parameters based on the Robust Optimization Model is proposed. This model is the robust counterpart of the least squares model, which is a Second Order Cone Program (SOCP), in which, possible uncertainties can reasonably be catered for [4]. Although SOCP has widely been used in operation research [5], to the authors' knowledge, this is the first attempt to apply this method to a geotechnical problem. However, before discussion of the proposed method, a brief review of some of the available approaches is presented.

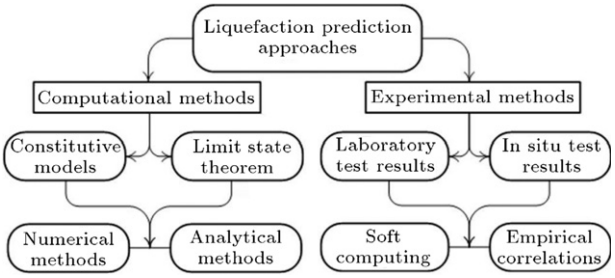

Figure 1: Classification of the approaches of lateral spreading predictions.

2. Review of the available methods

Following the concept presented in Figure 1, two basic approaches are described here; computational and experimental. In the latter approach, laboratory and/or field test results are used in conjunction with case histories to develop empirical correlations, whereas in computational methods, basic parameters are input into analytical or numerical models to predict the extent of the effect.

In recent years, new identification techniques have further enhanced the latter approach by providing fast and efficient codes for development of empirical models.

A brief review of each approach is provided here:

2.1. Computational based methods

Numerical and analytical methods have been widely used in geo-mechanics to simulate the patterns of kinematic behavior under various loadings. The success of such methods is highly dependent on the constitutive model and the input parameters.

The finite element or finite difference methods are perhaps the most widely used numerical methods. However, these procedures are highly dependent on material parameters that are usually difficult to estimate, and, as a result, limited success has been achieved in producing results that are comparable to field observations [6]. Numerical methods can also be utilized in conjunction with soft computing techniques to enhance or produce databases.

Analytical models have also contributed to the development of knowledge in this field. A number of simplified analytical models have been utilized to simulate liquefaction induced lateral spreading. The Sliding Block Model [7–10], Minimum Potential Energy Model [11,12], Shear Strength Loss and Strain Re-hardening Model [13], and the Viscous Model [14] are examples of this approach.

2.2. Experimental based methods

Due to the complexities of the phenomenon, the aforementioned constitutive models, as well as simplified analytical methods, have not succeeded in capturing the full effect. Thus, empirical models based on case histories have remained the more popular method in past decades.

Hamada et al. [15], Youd and Perkins [16], Bardet [13], Youd et al. [1] and Kanibir [17] introduced empirical correlations and Multi-Linear Regression (MLR) models for the assessment of liquefaction induced lateral spreading.

Al Bawwab [2] compiled a database of recorded cases of lateral spreading, used SPSS 2004 software for statistical analysis of the data and arrived at a number of correlations for

Table 1: Empirical correlations for prediction of the lateral displacement.

Method	Subset	Model	Limitations
Hamada et al. (1986)		$D_H = 0.75H^{1/2}\theta^{1/3}$	Number of case histories and variables
Youd and Perkins (1987)		$\text{Log}\, D_H = -3.49 - 1.86\text{Log}\, R + 0.98M_w$	Number of case histories and specific soil profile and topography conditions
Bardet et al. (1999)	Free-face	$\text{Log}\,(D_H + 0.01) = -17.372 + 1.248M_w - 0.923\text{Log}\, R - 0.014R + 0.685\text{Log}\, W + 0.3\text{Log}\, T_{15} + 4.826\text{Log}\,(100 - F_{15}) - 1.091D50_{15}$	Number of case histories and mistakes in databases that correct in youd models and uncertainty not assumed
	Slopping ground	$\text{Log}\,(D_H + 0.01) = -14.152 + 0.988M_w - 1.049\text{Log}\, R - 0.011R + 0.318\text{Log}\, S + 0.619\text{Log}\, T_{15} + 4.287\text{Log}\,(100 - F_{15}) - 0.705D50_{15}$	
Youd et al. (2002)	Free-face	$\text{Log}\, D_H = -16.713 + 1.532M_w - 1.406\text{Log}\, R^* - 0.012R + 0.592\text{Log}\, W + 0.540\text{Log}\, T_{15} + 3.413\text{Log}\,(100 - F_{15}) - 0.795\text{Log}\,(D50_{15} + 0.1\text{ mm})$	$5 \le W \le 20\%$ $6 \le M_W \le 8$, $0.1 \le S \le 6\%$, $1 \le T_{15} \le 15$ m, gravelly and/or very silty soils, critical depth up to 10 m
	Slopping ground	$\text{Log}\, D_H = -16.213 + 1.532M_w - 1.406\text{Log}\, R^* - 0.012R + 0.338\text{Log}\, S + 0.540\text{Log}\, T_{15} + 3.413\text{Log}\,(100 - F_{15}) - 0.795\text{Log}\,(D50_{15} + 0.1\text{ mm})$	
Kanibir (2003)	Free-face	$\text{Log}\, D_H = -20.71 + 25.32\text{Log}\, M_w - 1.39\text{Log}\, R^* - 0.009R + 1.15\text{Log}\, W + 0.19T_{15}0.5 - 0.02F_{15} - 0.84\text{Log}\,(D50_{15} + 0.1\text{ mm})$	Uncertainty not assumed
	Slopping ground	$\text{Log}\, D_H = -7.52 + 8.44\text{Log}\, M_w + 0.001R^* - 0.23R + 0.11S + 0.6\text{Log}\, T_{15} - 0.22F_{15} - 0.89\text{Log}\, D50_{15}$	
Al Bawwab (2005)	Model 1	$\text{Log}\, D_H = b_1 \cdot LSI + b_2 \cdot a_y/a_{\max} + b_3 \cdot \tan\beta/\tan\varphi' eqv, liq + b_4 \cdot z_{cr} + b_5 \cdot M_w + b_6 \cdot W + b_7$	Probabilistic analysis included
	Model 2	$\text{Log}\, D_H = b_1 \cdot LSI + b_2 \cdot a_y/a_{\max} + b_3 \cdot \tan\beta/\tan\varphi' eqv, liq + b_4 \cdot z_{cr} + b_5 \cdot M_w + b_6 \cdot \text{Log}\, S + b_7 \cdot \text{Log}\, W + b_8$	
	Model 3	$\text{Log}\, D_H = b_1 \cdot LSI + b_2 \cdot a_y/a_{\max} + b_3 \cdot \tan\beta/\tan\varphi' eqv, liq + b_4 \cdot \text{Log}\, z_{cr} + b_5 \cdot \text{Log}\, M_w + b_6 \cdot a_{\max} + b_7 \cdot \text{Log}\, S + b_8 \cdot \text{Log}\, W + b_9$	
	Model 4	$\text{Log}\, D_H = [(\theta_1 LSI + \theta_2)a_y/a_{\max} + (\theta_3 LSI + \theta_4)\tan\beta/\tan\varphi' eqv, liq + (\theta_5 LSI + \theta_6)\text{Log}\, z_{cr} + (\theta_7 LSI + \theta_8)\text{Log}\, M_w + (\theta_9 LSI + \theta_{10})a_{\max} + (\theta_{11} LSI + \theta_{12})\text{Log}\, S + (\theta_{13} LSI + \theta_{14})\text{Log}\, W + (\theta_{15} LSI + \theta_{16}) + \varepsilon]$	

determination of lateral displacement. In order to enhance the accuracy of the models, a maximum likelihood approach was considered and the effect of data uncertainty was taken into account by probabilistic methods.

Kramer and Baska [18] proposed a variation to the correlation presented by Youd et al. [1]. They established their model on a square root transformation of displacement rather than the logarithmic transformation used.

On a different note, Zhang et al. [19], based on empirical correlation on a cumulative shear strain model, introduced a "Lateral Displacement Index (LDI)" calculated by integration of maximum shear strain over potentially liquefiable layers, and then used it in a couple of simple correlations for "free-face" and "ground slope" cases. Idriss and Boulanger [20] used a different cumulative strain model to arrive at LDI.

Table 1 shows some of the empirical correlations found in the literature. The models proposed by Zhang et al. [19], Kramer and Baska [18] and Idriss and Boulanger [20] have not been included in this table, since they are directly comparable.

The difficulties posed by the fact that the phenomenon is dependent on multiple parameters have partly been alleviated by soft computing techniques, such as fuzzy logic, neuron computing, probabilistic reasoning and genetic algorithms. These methods of decision-making and optimization have firmly established themselves as indispensible tools for modeling natural phenomena.

Artificial Neural Networks (ANN) have been used for modeling seismically induced displacement, based on the same database used in the Multi Linear Regression model developed by Bartlet and Youd [21].

In the light of the above mentioned techniques, a new approach is proposed here, which combines the benefits of empirical models with an optimization method that considers the uncertainty of each parameter independently.

3. The proposed correlation

Following the trend proposed by Al Bawwab [2], $a_y/a_{\max}$, $\tan\beta/\tan\varphi' eqv$, liq and z_{cr} variables are used instead of T_{15}, F_{15}, and $D50_{15}$, which were used in some of the earlier models. This can be considered a step towards reaching a more descriptive group of variables and, consequently, a more powerful representative correlation. The descriptive variables are explained in Table 2, where a_y is the yield acceleration equal to $\tan(\varphi' eqv, liq\text{-}\beta)$ with finite slope assumption, and $\varphi' eqv, liq$ is the equivalent mobilized angle of internal friction of liquefied or potentially liquefiable soils [22,23].

Table 2: Deprive variables for predicting the lateral displacement.

Descriptive variables of a particular soil sub-layer.		
Seismological	M_W Duration of shaking	Moment magnitude scale of the earthquake [21,24–26]
	$a_{\max}$ Intensity of shaking	Maximum Horizontal Ground Acceleration (g)
Topographical	W Soil profile slope	Free-face ratio $= H/L(\%)$
	S Ground conditions	Ground Surface Slope (%)
	β Ground conditions	Ground surface slope angle (degrees) $= \tan^{-1}(S/100)$
Geotechnical	$\tan\phi' eqv, liq/\tan\beta$ Gravity force	FS against gravitational forces
	LSI Distribution of liquefaction potential through the depth	Liquefaction severity index
	$a_y/a_{\max}$ Sliding force	FS against sliding
	z_c Effective potentially liquefiable depth	Critical depth

Among the descriptive variables, there are two topological parameters (W and S), which refer to sloping sites without a free face (i.e. $W = 0$) and level sites with a free face (i.e. $S = 0$) as in Figure 2.

With these definitions, case histories can be divided into two subsets of sloping sites without a free face and non-sloping sites with a steep face [1,2,17].

Table 3: Sample of the database.

	D_H	M_w	$a_{max/g}$			S	W	LSI			Zcr			a_y/a_{max}			$\tan\beta/\tan\varphi'$			Earthquake
1	1	7.9	0.6	±	0.15	0.6	0	3.55	±	0.89	3.5	±	0.88	0.07	±	0.026	0.124	±	0.03	1906 San Francisco–USA [1]
2	1.09	7.5	0.19	±	0.05	0.31	0	5.8	±	0.09	1.09	±	0.08	0.264	±	0.09	0.058	±	0.013	1964 Niigata–Japan [1]
3	1.37	9.2	0.21	±	0.05	0.7	7.03	6.18	±	1.55	4.57	±	1.14	0.594	±	0.168	0.053	±	0.007	1964 Alaska [1]
4	1.68	6.4	0.55	±	0.14	1.23	0	0.01	±	0	11.89	±	2.97	1.488	±	0.373	0.015	±	0	1971 San Fernando–USA [1]
5	0	7.5	0.12	±	0.03	3.5	1.03	1.25	±	0.31	5.56	±	1.39	0.864	±	0.256	0.252	±	0.03	1976 Guatemala [23]
6	1	7.4	0.2	±	0.05	1	0	0.96	±	0.24	12.19	±	3.05	0.537	±	0.158	0.085	±	0.012	1977 Argentina [27]
7	0.86	6.5	0.51	±	0.13	2	4.69	1.65	±	0.16	3.36	±	1.55	0.406	±	0.107	0.088	±	0.006	1979 Imperial Valley–USA [1]
8	0	6.9	0.6	±	0.15	11	0	2.06	±	0.52	1.74	±	0.44	0	±	0.027	1.392	±	0.152	1983 Borah Peak–USA [1]
9	1.14	7.7	0.25	±	0.06	0.56	0	3.01	±	0.75	3	±	0.75	0.567	±	0.157	0.038	±	0.004	1983 Nihonkai-Chubu–Japan [1]
10	0.2	6.6	0.21	±	0.05	0.47	41.38	1.94	±	0.48	3.05	±	0.76	0.345	±	0.117	0.061	±	0.013	1988 Superstition Hills–USA [1]
11	0.5	7	0.13	±	0.03	0	10	1.11	±	0.28	6.34	±	1.59	0.717	±	0.22	0	±	0	1989 Loma Prieta–USA [1]
12	5	7.6	0.2	±	0.05	0.5	50	7.73	±	1.93	9.23	±	2.31	0.249	±	0.085	0.091	±	0.019	1990 Luzon–Phillipines [28]
13	1	6.7	0.52	±	0.13	1	0	0	±	0	14.1	±	3.53	2.718	±	0.68	0.007	±	0	1994 Northridge–USA [1]
14	0.4	6.9	0.6	±	0.15	0.1	0	5.08	±	1.27	13.5	±	3.38	0.358	±	0.094	0.005	±	0	1995 Hyogoken-Nambu–Japan [1]
15	5.84	7.6	0.43	±	0.11	1	5	3.47	±	0.87	2.8	±	0.7	0.118	±	0.04	0.165	±	0.032	1999 Chi Chi–Taiwan [29]
16	2.2	7.4	0.4	±	0.1	1.6	0	4.54	±	1.14	9.8	±	2.45	0.138	±	0.054	0.225	±	0.053	1999 Kocaeli (Izmit)–Turkey [30]
17	0.3	6.5	0.12	±	0.03	1	0	0.56	±	0.14	2.75	±	0.69	0.371	±	0.134	0.183	±	0.039	2003 San Simeon–USA [31]
18	0.2	7.9	0.31	±	0.08	0.1	0	2.29	±	0.57	11	±	2.75	0.368	±	0.106	0.009	±	0.001	2003 Tokachi-Oki–Japan [32]

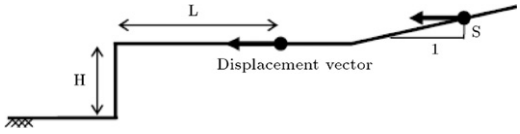

Figure 2: Topography related descriptive variables.

In order to provide bases for comparison of the efficiency of the models under various uncertainties, the first three correlations proposed by Al Bawwab [2] are used in this study. Due to the fact that the parameters of the fourth correlation are in multiple forms, the concept of multiple uncertainties could not be defined. Thus, the fourth correlation was substituted by a slightly different linear correlation. Furthermore the correlations are cast into the two aforementioned geometrical sub-sets:

Model 1:

$$W = 0 \quad \text{Log}\, D_H = a_1 M_w + a_2 S + a_3 LSI + a_4 Zcr + a_5 a_y/a_{\max} + a_6 \tan\beta/\tan\varphi' + a_7$$
$$S = 0 \quad \text{Log}\, D_H = a_1 M_w + a_2 W + a_3 LSI + a_4 Zcr + a_5 a_y/a_{\max} + a_6 \tan\beta/\tan\varphi' + a_7.$$

Model 2:

$$W = 0 \quad \text{Log}\, D_H = a_1 M_w + a_2 \text{Log}\, S + a_3 LSI + a_4 Zcr + a_5 a_y/a_{\max} + a_6 \tan\beta/\tan\varphi' + a_7$$
$$S = 0 \quad \text{Log}\, D_H = a_1 M_w + a_2 \text{Log}\, W + a_3 LSI + a_4 Zcr + a_5 a_y/a_{\max} + a_6 \tan\beta/\tan\varphi' + a_7.$$

Model 3:

$$W = 0 \quad \text{Log}\, D_H = a_1 \text{Log}\, M_w + a_2 a_{max/g} + a_3 \text{Log}\, S + a_4 LSI + a_5 \text{Log}\, Zcr + a_6 a_y/a_{\max} + a_7 \tan\beta/\tan\varphi' + a_8$$
$$S = 0 \quad \text{Log}\, D_H = a_1 \text{Log}\, M_w + a_2 a_{max/g} + a_3 \text{Log}\, W + a_4 LSI + a_5 \text{Log}\, Zcr + a_6 a_y/a_{\max} + a_7 \tan\beta/\tan\varphi' + a_8.$$

New Linear Model:

$$W = 0 \quad D_H = a_1 M_w + a_2 a_{max/g} + a_3 S + a_4 LSI + a_5 Zcr + a_6 a_y/a_{\max} + a_7 \tan\beta/\tan\varphi' + a_8$$
$$S = 0 \quad D_H = a_1 M_w + a_2 a_{max/g} + a_3 W + a_4 LSI + a_5 Zcr + a_6 a_y/a_{\max} + a_7 \tan\beta/\tan\varphi' + a_8.$$

Since it is important to evaluate the effect of each coefficient separately, the correlations are cast into matrix form, $Ax = b$, where $A_{m\times n}$, $(m > n)$ and $b_{n\times 1}$.

Classical regression analysis is:

$$\min \|A_x - b\|. \quad (1)$$

However, this approach does not provide for various degrees of uncertainty and, thus, a more versatile approach is called for, which is discussed in the following section.

In order to examine the potentials of each of the correlations, the database compiled by Youd et al. [1], including 1906 San Francisco–USA, 1964 Prince William Sound–Alaska, 1964 Niigata–Japan, 1971 San Fernando–USA, 1979 Imperial Valley–USA, 1983 Borah Peak–USA, 1983 Nihonkai-Chubu–Japan, 1987 Superstition Hills–USA, 1989 Loma Prieta–USA, and 1995 Hyogoken-Nanbu–Japan, and 91 case histories from 7 different earthquakes added by Al Bawwab [2], including the 1976 Guatemala, 1977 San Juan-Argentina, 1990 Luzon–Philippines, 1994 Northridge–USA, 1995 Hyogoken-Nanbu-Japan, 1999 Kocaeli (Izmit)–Turkey, 1999 Chi Chi–Taiwan, 2003 San Simeon-USA earthquake and 2003 Tokachi-Oki–Japan earthquakes, is used. The distribution of descriptive variable characteristics for all case histories has been shown in Figure 3.

In Table 3, a sample of the data is presented. As noted previously [2], the data contain uncertainty and, thus, the associated variation must be considered in any evaluation, which is not directly possible in the MLR analysis.

4. Robust optimization model

In mathematical optimization models, it is commonly assumed that the data inputs are precise and the influence of parameter uncertainties on the optimality and feasibility of the models are ignored. It is, therefore, conceivable that as the data differ from the assumed nominal values, the generated optimal solution may violate critical constraints and perform poorly from an objective function point of view. These observations motivate the need for methodologies in mathematical optimization models that account for solutions immune to data uncertainty [4,5]. For example, inaccuracies enter in the field measurements of lateral displacement or critical depth in case histories, just as all other natural phenomenon measurements. Such inaccuracies exist in other influencing parameters and can cause deviation. If such deviations are presented as boundaries of the central point of the data (Figure 4), and the true data point could exist at any point within this boundary, the Robust Optimization

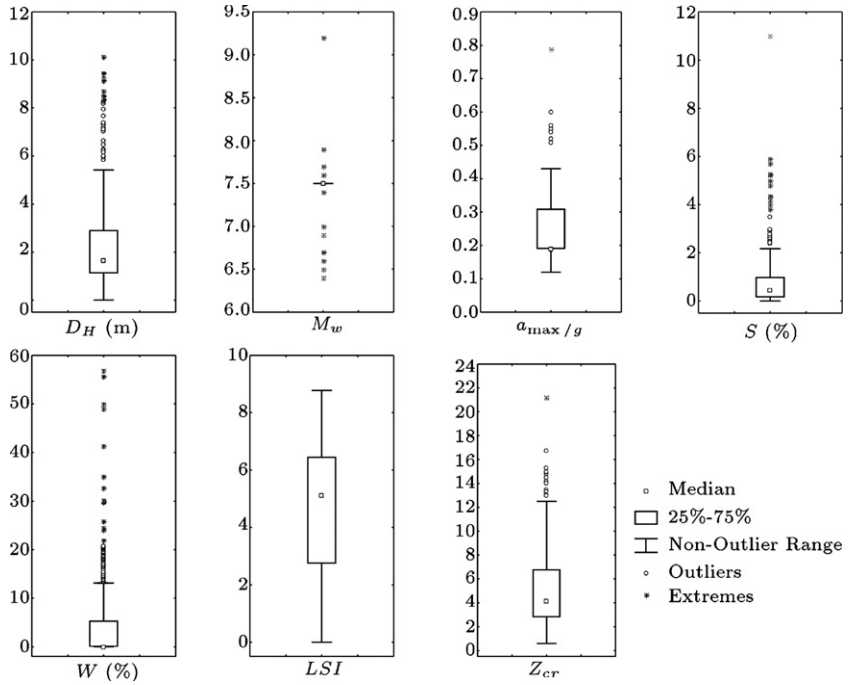

Figure 3: Distribution of descriptive variable characteristics for all case histories.

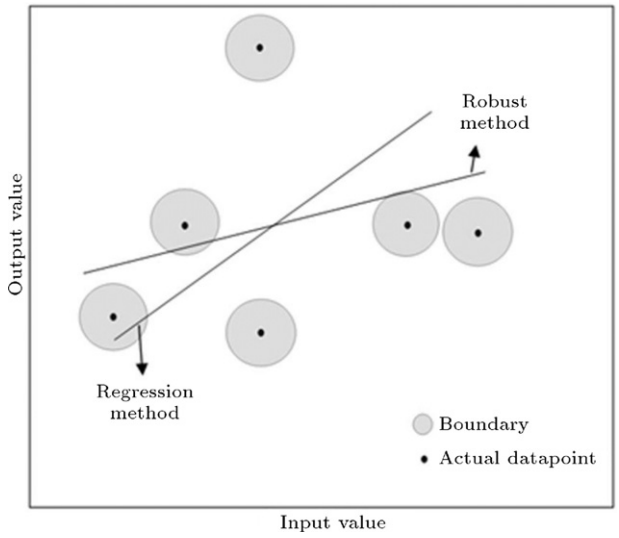

Figure 4: Robust and regression methods.

seeks to minimize maximum error with any particular level of uncertainty. In the particular case of zero uncertainty, this approach reduces to least squares analysis [33].

In the past decade, there have been considerable developments in the theory of robust convex optimization. However, under the robust framework found in the literature, the robust models generally lead to an increase in computational complexity over the nominal problem, which is an issue when solving large problems [4,5].

In the sequel, a robust model for the least squares method is presented. Supposing that the level of uncertainty of databases is known and it is equal to ρ. Then, the robust model minimizes the worst case residual, i.e:

$$\min_{x} \max_{\|[E,r]\|_F \le \rho} \|(A+E)\,x - (b+r)\|\,, \tag{2}$$

where E and r are uncertainties in A and b, respectively and the matrix norm is the Frobenius norm, which, for a given matrix, A, is defined as $\|A\|_F = \left(\sum_i^n \sum_j^m A_{ij}^2\right)^{\frac{1}{2}}$. Obviously, the problem Eq. (2) cannot be solved using classical optimization algorithms. However, it can be written in the following Second Order Conic Programming (SOCP) form [34]:

$$\begin{cases} \min\,(t+\rho s) \\ \|A_x - b\| \le t \\ \sqrt{1+\|x\|^2} < s \end{cases} \tag{3}$$

and solved using efficient software like SeDuMi [35], which is an interior point based software for solving SOCP and semi definite optimization. It may be noted from an unconstrained least squares problem, a SOCP is developed that is harder to solve, but is more conservative.

Thus, the problem Eq. (3) is rewritten in the dual form of SeDuMi's input format, namely:

$$\begin{cases} \max b^T y \\ c - A^t y \in K \end{cases} \tag{4}$$

where:

$$c = \begin{pmatrix} 0 \\ -b \\ 0 \\ 1 \\ 0_{n\times 1} \end{pmatrix}, \quad A^t = \begin{pmatrix} -1 & 0 & 0_{1\times n} \\ 0_{m\times 1} & 0_{m\times 1} & -A \\ 0 & -1 & 0_{1\times n} \\ 0 & 0 & 0_{1\times n} \\ 0_{n\times 1} & 0_{n\times 1} & -I_{n\times n} \end{pmatrix}, \quad b = \begin{pmatrix} -1 \\ -\rho \\ 0_{n\times 1} \end{pmatrix}, \quad Y = \begin{pmatrix} t \\ s \\ x \end{pmatrix}, \tag{5}$$

$$K = Q_{m+1} \times Q_{n+2}, \tag{6}$$

where Q_k denotes the second order cone in R^k and is defined as follows:

$$Q_k = \left\{x \in R^k |\, \|\bar{x}\| \le x_1\right\}, \quad \bar{x} = (x_1, \ldots, x_{k-1})^T. \tag{7}$$

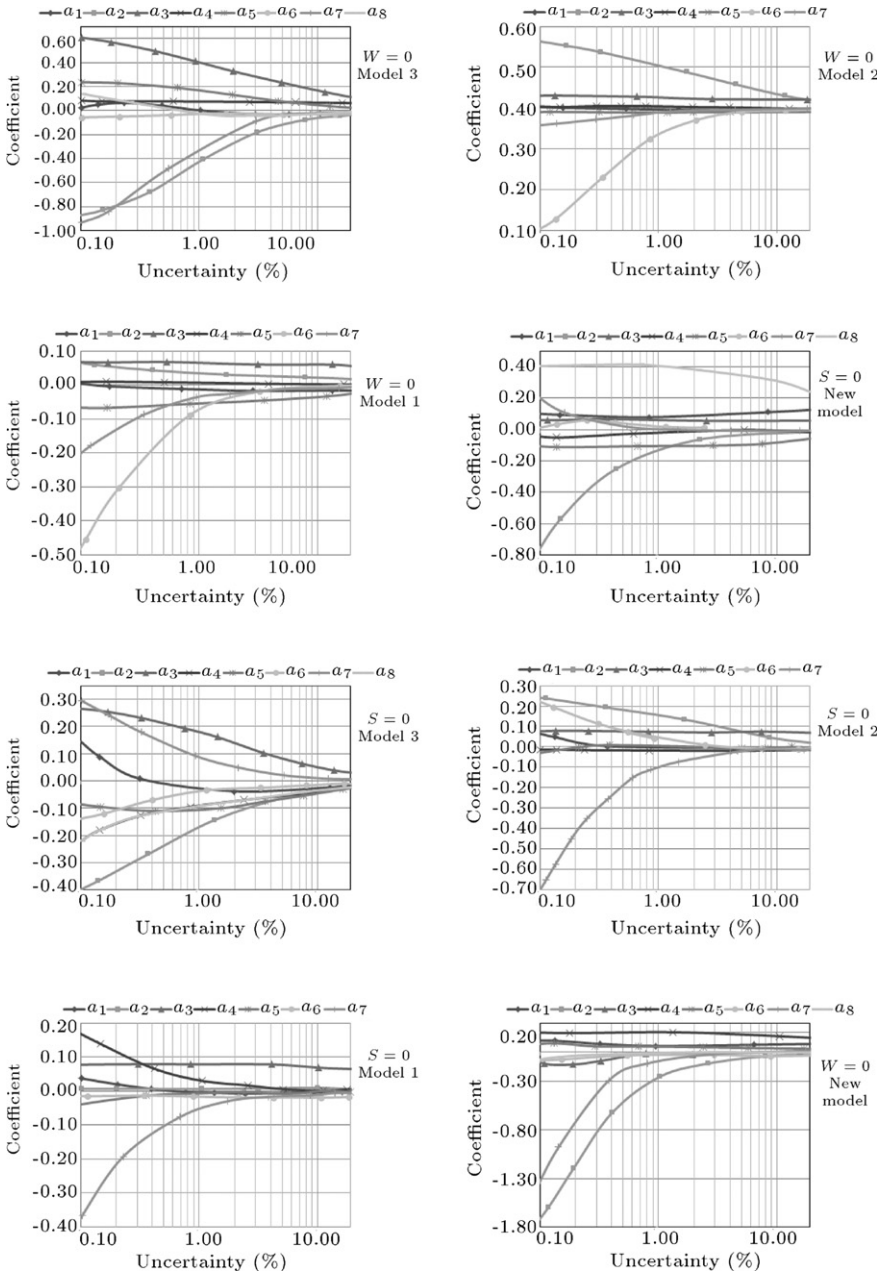

Figure 5: Variation of constant coefficients of different models, versus uncertainties.

By this definition, one now can easily see that the first constraint in Eq. (3) belongs to Q_{m+1} and the second one belongs to Q_{m+2}. These are denoted in SeDuMi's format by the product of these two second order cones, namely K.

Then, SeDuMi is called by the following command for four different values of uncertainty parameter ρ:

$$[x, y] = sedumi(At, b, c, K), \tag{8}$$

where At denotes the matrix, A^t, in Eq. (5). b, c also are taken from Eq. (5) and K also is given by Eq. (6). Moreover, x and y denote the solutions of Eq. (4) and their dual problem.

In order to consider uncertainty, a new parameter is introduced:

$$Uncertainity = \frac{\rho}{\|Data\|_F} \times 100, \tag{9}$$

Table 4: The most sensitive coefficients.

Models	Topological condition	
	Free face	Gently sloping
Model 1	a7	a7
Model 2	a7	a2
Model 3	a2	a2 & a7
The new model	a2	a2 & a7

where $\|Data\|_F$ is the Frobenius norm of data matrices, as defined before.

Using Eq. (9), the uncertainty of the matrices for the two topological conditions were evaluated to be 10.33% for free face and 17.08% for the gently sloping condition. In other words, the matrix of error or uncertainty ($\pm$ values) has been formed

Table 5: Constants coefficient for each model by uncertainties.

	$S = 0$				$W = 0$			
	Model 1	Model 2	Model 3	New model	Model 1	Model 2	Model 3	New Model
a1	−0.0034	−0.0042	−0.0258	0.1298	−0.0143	−0.0109	−0.0191	0.0934
a2	0.0053	0.0441	−0.0424	−0.0121	0.0214	0.0708	−0.0421	−0.0138
a3	0.0707	0.0733	0.0527	0.0617	0.059	0.0598	0.1244	0.0338
a4	−0.0169	−0.0151	0.0706	0.2991	0.0046	0.0054	0.0592	0.1727
a5	−0.0023	−0.0018	−0.0483	−0.0756	−0.0236	−0.0232	0.024	0.0559
a6	0.0028	0.0037	−0.0149	−0.001	−0.0023	−0.0011	−0.0353	−0.0095
a7	−0.0061	−0.0087	0.011	0.0008	−0.0043	−0.0039	−0.0097	−0.0009
a8	–	–	−0.0388	0.0129	–	–	−0.0242	0.0103
R^2(%)	**54**	**68**	**68**	**71**	**81**	**82**	**83**	**83**

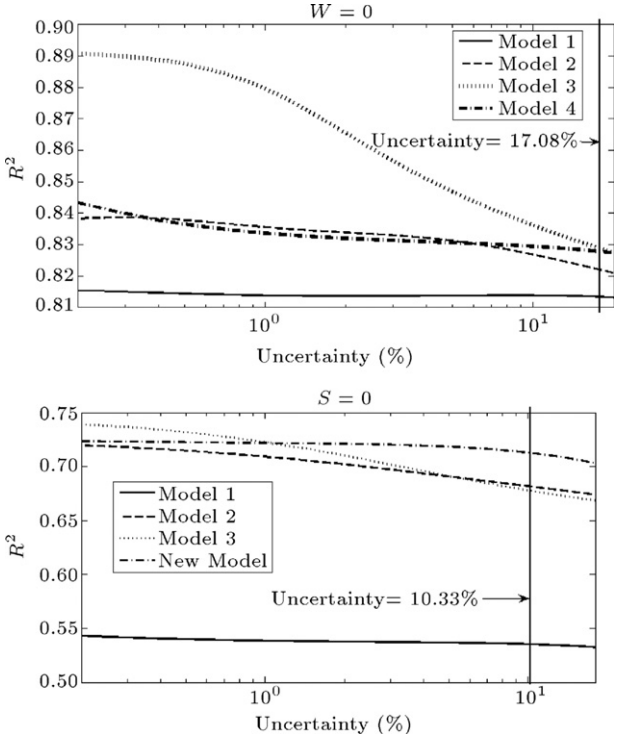

Figure 6: Variation of regression coefficient (R^2) of different models, versus uncertainties.

and the Frobenius norm of the matrix of error divided into the Frobenius norm of the data matrix (without ± values).

5. The results

As stated earlier, optimization of the coefficients is the main task of this paper. Thus, the variations of the coefficients were evaluated against various levels of uncertainty for the two topological condition of free-face and gently sloping. The results are summarized in Figure 5.

These figures show that by increasing the uncertainty, the variability approaches a stable value.

The above figures constitute a sensitivity analysis for each coefficient of the variables against levels of uncertainty. In other words, the coefficients with greater variations show that their respective variables have greater sensitivity. The most sensitive coefficients are presented in Table 4.

It must be pointed out at this stage that if uncertainty (%) is set to zero, the method reduces to an ordinary MLR technique.

It can be noted that parameters $a_{\max/g}$ and $\tan\beta/\tan\varphi'$ are most sensitive.

In order to determine the accuracy of each model, the statistical value of R^2, as an absolute fraction of variance, can be used, defined as follows [36]:

$$R^2 = 1\left[\frac{\sum_{i=0}^{M}(Y_{i(Model)} - Y_{i(Actual)})^2}{\sum_{i=1}^{M}(Y_{i(Actual)})^2}\right]. \quad (10)$$

The response of each model to various levels of uncertainty is shown in Figure 6.

These figures show that while the aforementioned models can provide reasonably good predictions for cases in which uncertainties are neglected, their applications to cases with high uncertainty cannot provide the same levels of accuracy. Under each sub-set, the proposed approach achieves better predictions with assumed uncertainties, and at mentioned uncertainty, the predictions of the new correlation supersedes other correlations.

Based on the approach presented in this study, the most optimum coefficients for each of the above mentioned models (with the aforementioned levels of uncertainty) are presented in Table 5 and Figure 7.

6. Conclusions

Avoidance of uncertainty in any statistical analysis of natural phenomenon such as lateral spreading is impossible. MLR methods alone cannot cater for this effect and, thus, probabilistic approaches are required.

In this study, a robust optimization method is developed for evaluation of the effect of uncertainty of each parameter independently on the outcome of analysis. This is a step forward in comparison with limited probabilistic approaches that considers the variation of parameters singularly.

A new parameter was introduced to express the levels of uncertainty of the data. Also, for the dataset used, minimum percentages of uncertainty, for which the proposed correlation performs better, were evaluated for the two conditions of free face and gently sloping, to be 10.33% and 17.08%, respectively.

The use of the robust optimization method allows evaluation of the sensitivity of parameter coefficients against uncertainty. This analysis determined the most sensitive parameters to uncertainty. It was shown that for models 1 and 2 of the free face condition, the constant coefficient (a7) was the most sensitive coefficient, which is an indication of the unsuitability of the models. For the other two models under the same geometrical condition, the coefficient of $a_{\max/g}$ variable (a2) is the most sensitive, which is as expected.

For the gently sloping condition, the constant coefficient of the first model (a7), the coefficient of slope ($\mathrm{Log}\,S$) (a2) in model 2, and for the other models, coefficients of $a_{\max/g}$

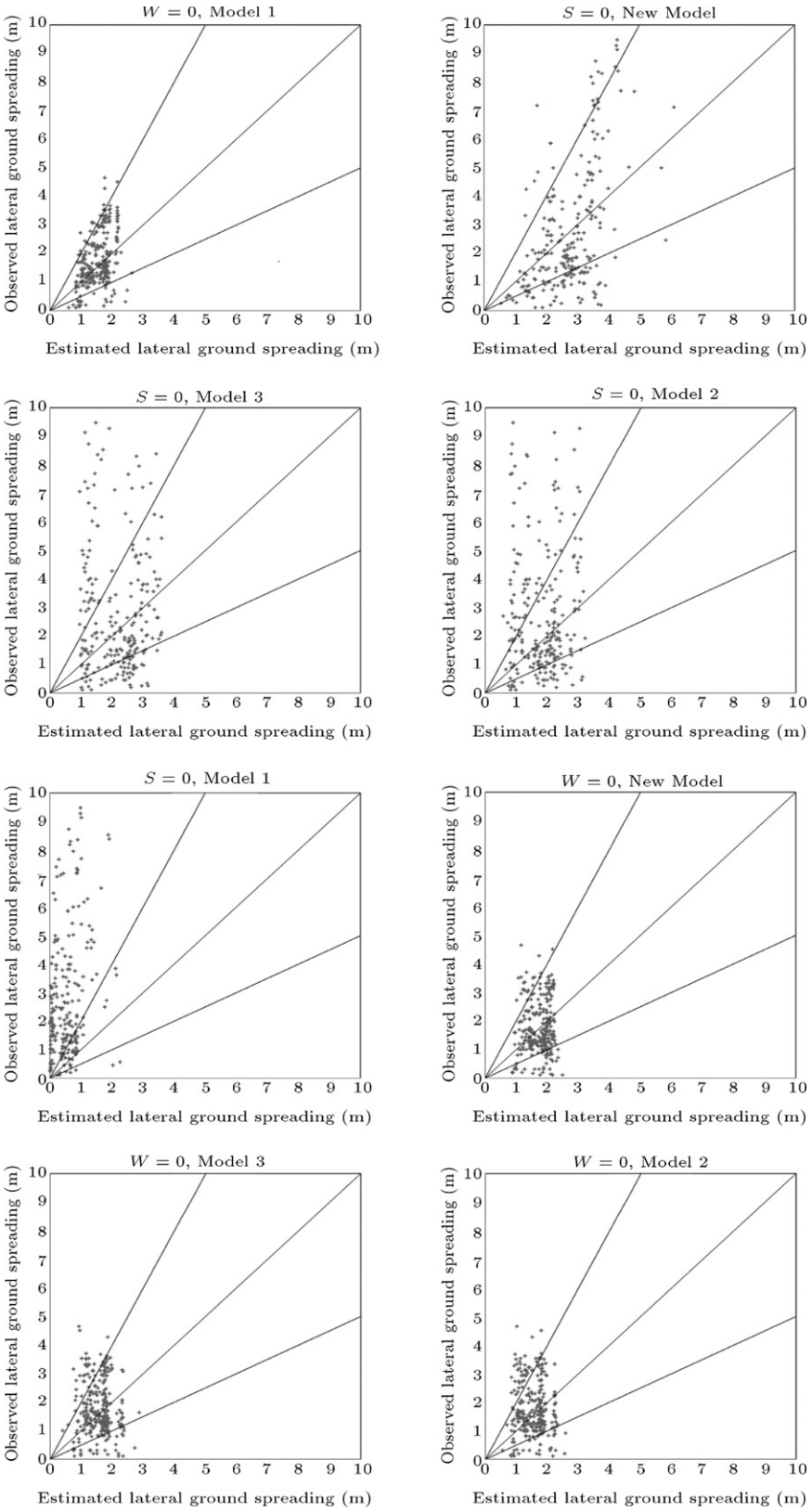

Figure 7: Validation of different models in acceptable uncertainties.

and $\tan\beta/\tan\varphi'$, are the most sensitive. It may, thus, be concluded that the latter two models are performing logically, since the two important variables have the greatest effect on the outcome.

Statistical comparison of the models shows that under very small values of uncertainty, the accuracy of model 3 is particular, and logarithmic models in general are better. However, under high levels of data uncertainty (in particular the aforementioned parameters), the new linear model performs better, and based on this approach, the most optimum values for each coefficient of each model was calculated and fed into the model for prediction of lateral spreading. Needless to say, this model reverts to ordinary regression analysis in the absence of uncertainty.

References

[1] Youd, T.L., Hansen, C.M. and Bartlett, S.F. "Revised multi-linear regression equations for prediction of lateral spread displacement", *Journal of Geotechnical and Geoenvironmental Engineering, ASCE*, 128(12), pp. 1007–1017 (2002).

[2] Al Bawwab, W.M. "Probabilistic assessment of liquefaction-induces lateral ground deformations", Ph.D. Thesis (C. Özgen. Advisor), Department of Civil Engineering, Middle East Technical University (2005).

[3] Baziar, M.H. and Ghorbani, A. "Evaluation of lateral spreading using artificial neural networks", *Soil Dynamics and Earthquake Engineering*, 25(1), pp. 1–9 (2005).

[4] Alizadeh, F. and Goldfarb, D. "Second order cone programming", *Mathematical Programming, Series B*, 95, pp. 3–51 (2003).

[5] Soma Lobo, M., Vanderberghe, L., Boyd, S. and Lebret, H. "Applications of second-order cone programming", *Linear Algebra and its Applications*, 284, pp. 193–223 (1998).

[6] Javadi, A.A., Rezania, M. and MousaviNezhad, M. "Evaluation of liquefaction induced lateral displacements using genetic programming", *Computers and Geotechnics*, 33(4–5), pp. 222–233 (2006).

[7] Newmark, N.M. "Effects of earthquakes on embankments and dams", *Géotechnique*, 15(2), pp. 139–160 (1965).

[8] Yegian, M.K., Marciano, E.A. and Gharaman, V.G. "Earthquake-induced permanent deformation: probabilistic approach", *Journal of Geotechnical and Geoenvironmental Engineering, ASCE*, 117(1), pp. 35–50 (1991).

[9] Baziar, M.H., Dobry, R. and Elgamal, A.W.M. "Engineering evaluation of permanent ground deformation due to seismically-induced liquefaction", Technical Report No. NCEER-92-0007, National Center for Earthquake Engineering Research, State University of New York, Buffalo (1992).

[10] Jibson, R.W. "Predicting earthquake-induced landslide displacement using newmark's sliding block analysis", In *Transportation Research Record 1411*, pp. 9–17, Transportation Research Board, Washington D.C. (1994).

[11] Towhata, I., Sasaki, Y., Tokida, K.I., Matsumoto, H., Tamari, Y. and Yamada, K. "Prediction of permanent displacement of liquefied ground by means of minimum energy principle", *Soils and Foundations*, 32(2), pp. 97–116 (1992).

[12] Tokida, K., Matsumoto, H., Azuma, T. and Towhata, I. "Simplified procedure to estimate lateral ground flow by soil liquefaction", *Journal of Soil Dynamics and Earthquake Engineering*, 3(1), pp. 381–396 (1993).

[13] Bardet, J.P., Mace, N. and Tobita, T. "Liquefaction-induced ground deformation and failure, a report to PEER/PG&E. Task 4A - Phase 1", Civil Eng Dep., University of Southern California, Los Angeles (1999).

[14] Hamada, M., Sato, H. and Kawakami, T.A. "Consideration for the mechanism for liquefaction-related large ground displacement", *Proceedings of the 5th U.S. Japan Workshop on Earthquake Resistant Design of Lifeline Facilities and Countermeasures for Soil Liquefaction*, NCEER Report 94-0026, pp. 217–232 (1994).

[15] Hamada, M., Yasuda, R. and Isoyama, S. "Study on liquefaction induced permanent ground displacement", Report for the Association for the Development of Earthquake Prediction, Japan (1986).

[16] Youd, T.L. and Perkins, D.M. "Mapping of liquefaction induced ground failure potential", *Journal of the Geotechnical Engineering Division, ASCE*, 104, pp. 433–446 (1987).

[17] Kanibir, A. "Investigation of the lateral spreading at sapanca and suggestion of empirical relationships for predicting lateral spreading", M.Sc. Thesis, Department of Geological Engineering, Hacettepe University, Ankara, Turkey (2003) (in Turkish).

[18] Kramer, S.L. and Baska, D.A. "Estimation of permanent displacements due to lateral spreading", *Journal of Geotechnical and Geoenvironmental Engineering, ASCE*, 111(6), pp. 772–792 (2007).

[19] Zhang, G., Robertson, K.P. and Brachman, I.W.R. "Estimating liquefaction-induced lateral displacements using the standard penetration test or cone penetration test", *Journal of Geotechnical and Geoenvironmental Engineering, ASCE*, 130(8), pp. 861–871 (2004).

[20] Idriss, I.M. and Boulanger, R.W. "Soil liquefaction during earthquakes", In *EERI Monograph, 12*, p. 262. Earthquake Engineering Research Institute, California (2008).

[21] Bartlett, S.F. and Youd, T.L. "Empirical analysis of horizontal ground displacement generated by liquefaction-induced lateral spreads", Technical Report No. NCEER-92-0021, National Center for Earthquake Engineering Research, State University of New York, Buffalo, pp. 5–15 (1992).

[22] Stark, T.D. and Mesri, G. "Undrained shear strength of liquefied sands for stability analysis", *Journal of Geotechnical and Geoenvironmental Engineering, ASCE*, 118(11), pp. 1727–1747 (1992).

[23] Seed, H.B., Arango, I., Chan, C.K., Gomez-Masso, A. and Ascoli, R.G. "Earthquake-induced liquefaction near lake Amatitlan, Guatemala", Report No. UCB/EERC-79/27 (1979).

[24] Housner, G.W. "Intensity of earthquake ground shaking near the causative fault", *Proceedings of the 3rd World Conference on Earthquake Engineering*, 3, Auckland, pp. 94–119 (1965).

[25] Trifunac, M.D. and Brady, A.G. "A study on the duration of strong earthquake ground motion", *Bulletin of the Seismological Society of America*, 65(3), pp. 581–626 (1975).

[26] Das, B.M., *Principles of Soil Dynamics*, p. 592. Thomson-Engineering (1992).

[27] Rojahn, C., Brogan, G.E. and Siemmons, D.B. "Preliminary report on the San Juan, Argentina earthquake of November 23, 1977", U.S. Geological Survey, Menlo Park, CA, USA (1977).

[28] Tokimatsu, K., Kojima, H., Kuwayama, S., Abe, A. and Midorikawa, S. "Liquefaction-induced damage to buildings in 1990 Luzon earthquake", *Journal of Geotechnical and Geoenvironmental Engineering, ASCE*, 120(2), pp. 290–307 (1992).

[29] Juang, H. "Soil Liquefaction in the 1999 Chi-Chi, Taiwan, earthquake", Clemsom University website: www.ces.clemson.edu/chichi/TW-LIQ.

[30] Cetin, K.O., Youd, T.L., Seed, R.B., Bray, J.D., Sancio, R., Lettis, W., Tolga, M.T. and Durgunoglu, H.T. "Liquefaction-induced ground deformations at hotel Sapanca during Kocaeli (Izmit)–Turkey Earthquake", *Soil Dynamics and Earthquake Engineering*, 22, pp. 1083–1092 (2002).

[31] Holzer, T., Noce, T.E., Bennett, M.J., Alessandro, C., Boatwrite, J., Tinsley, J.C., Sell, R.W. and Rosenberg, L.I. "Liquefaction-induced lateral spreading in Oceano, California, during the 2003 San Simeon earthquake", USGS Open-File Report No. 2004–1269, Version 1.0 (2004).

[32] Sasajima, T., Kabouchi, A., Kohama, E., Watanabe, J., Miura, K. and Otsuka, N. "Liquefaction induced deformation of test quay wall in Kushiro port during the 2003 Tokachi-oki earthquake", Geo-Frontiers (2005).

[33] Mola-abasi, H. "Liquefaction zonation in Golestan province of Iran with evaluation of lateral spreading", M.Sc. Thesis (F. Kalantary. Advisor), Department of Civil Engineering, University of Guilan (2010).

[34] Wang, B. "Implementation of interior point methods for second order conic optimization", M.Sc. Thesis, MacMaster University, Hamilton, Canada (2003).

[35] Sturm, J.F. "Using SeDuMi 1.02. a MATLAB toolbox for optimization over symmetric cones", In *Optimization Methods and Software, 11*, pp. 625–653, Taylor and Francis (1999).

[36] Nariman-Zadeh, N., Darvizeh, A. and Ahmad-Zadeh, G.R. "Hybrid genetic design of GMDH-type neural networks using singular value decomposition for modelling and prediction of the explosive cutting process", *Proc. I MECH E Part B J. Eng.Manufact.*, 217, pp. 779–90 (2003).

Farzin Kalantary received his BS degree from Wales, UK, his MS degree from Cardiff University, UK, and his Ph.D. degree in soil and powder mechanics from Wales, Swansea University, UK. He joined the Department of Civil Engineering at the University of Guilan, Iran, in 1992-93, and offered basic and advanced courses in civil and mechanical engineering, in computational geomechanics and numerical modeling. He moved to the K.N.T. University of Technology, Tehran, Iran, in 2008, where he is serving as one of the faculty members in the Department of Geotechnical Engineering. His main research interests include: soil plasticity, soil and rock constitutive modeling, and application of numerical methods in soil mechanics, etc. He has published some books and papers in this area.

Hossein MolaAbasi received his BS degree in Water Engineering and MS degree in Geotechnical Engineering from Ferdowsi University of Mashhad, Iran, and the University of Guilan, Iran, in 2003 and 2005, respectively. He is currently taking his Ph.D. program in Geotechnical Engineering at Babol University of Technology, Iran, under the supervision of Dr. Shooshpasha. His main research interests include: soft computing modeling in soil and rock mechanics.

Maziar Salahi received his MS degree in Applied Mathematics from Sharif University of Technology, Tehran, Iran, and a Ph.D. degree in Applied Mathematics, Optimization, from McMaster University, Canada. His primary research interests are: interior point methods for linear and nonlinear optimization problems, conic optimization and integer programming.

Mehdi Veiskarami was born in Tehran, Iran. He received his BS degree in Civil Engineering and MS degree in Geotechnical Engineering from the University of Guilan, Iran, in 2003 and 2005, respectively. He also received his Ph.D. degree in Geomechanics from Shiraz University in 2010. Dr. Mehdi Veiskarami joined the Department of Civil Engineering at the University of Guilan in 2010, where he currently serves as Assistant Professor. His main research areas include: computational modeling in soil and rock mechanics. He has published some papers and a book, which are mainly focused on theoretical aspects of Geomechanics.